The Journal of Immunology

IL-23–Independent Induction of IL-17 from γδT Cells and Innate Lymphoid Cells Promotes Experimental Intraocular Neovascularization

Eiichi Hasegawa, Koh-Hei Sonoda, Takashi Shichita, Rimpei Morita, Takashi Sekiya, Akihiro Kimura, Yuji Oshima, Atsunobu Takeda, Takeru Yoshimura, Shigeo Yoshida, Tatsuro Ishibashi and Akihiko Yoshimura

J Immunol 2013; 190:1778-1787; Prepublished online 14 January 2013;
doi: 10.4049/jimmunol.1202495
http://www.jimmunol.org/content/190/4/1778

The Journal of Immunology is published twice each month by
The American Association of Immunologists, Inc.,
1451 Rockville Pike, Suite 650, Rockville, MD 20852

Print ISSN: 0022-1767 Online ISSN: 1550-6606.

IL-23–Independent Induction of IL-17 from γδT Cells and Innate Lymphoid Cells Promotes Experimental Intraocular Neovascularization

Eiichi Hasegawa,*,†,‡ Koh-Hei Sonoda,§ Takashi Shichita,*,† Rimpei Morita,*,† Takashi Sekiya,*,† Akihiro Kimura,*,† Yuji Oshima,‡ Atsunobu Takeda,‡ Takeru Yoshimura,‡ Shigeo Yoshida,‡ Tatsuro Ishibashi,‡ and Akihiko Yoshimura*,†

Choroidal neovascularization (CNV) is a characteristic of age-related macular degeneration. Genome-wide association studies have provided evidence that the immune system is involved in the pathogenesis of age-related macular degeneration; however, the role of inflammatory cytokines in CNV has not been established. In this study, we demonstrated that IL-17 had a strong potential for promoting neovascularization in a vascular endothelial growth factor–independent manner in laser-induced experimental CNV in mice. Infiltrated γδT cells and Thy-1$^+$ innate lymphoid cells, but not Th17 cells, were the main sources of IL-17 in injured eyes. IL-23 was dispensable for IL-17 induction in the eye. Instead, we found that IL-1β and high-mobility group box 1 strongly promoted IL-17 expression by γδT cells. Suppression of IL-1β and high-mobility group box 1, as well as depletion of γδT cells, reduced IL-17 levels and ameliorated experimental CNV. Our findings suggest the existence of a novel inflammatory cytokine network that promotes neovascularization in the eye. ***The Journal of Immunology*****, 2013, 190: 1778–1787.**

Age-related macular degeneration (AMD) is the leading cause of irreversible visual impairment in persons aged 60 y and older in Western countries (1). The pathogenesis of AMD is complex and not well established. Chronic local inflammation from persistent infection was recently identified as a candidate etiology for AMD. Choroidal neovascularization (CNV), the hallmark of wet AMD, was shown to be dependent on inflammatory cytokines, as well as inflammatory signals. Genetic studies also demonstrated strong associations between AMD and several gene variants in genes coding for inflammatory mediators and complement proteins (1–3).

CNV consists of new blood vessel growth from the choroid extending into the subretinal space. These immature vessels easily permit subretinal bleeding or extravascular leakage of blood components, causing injury to the retina. Vascular endothelial growth factor (VEGF) from retinal pigment epithelium (RPE) cells and infiltrating macrophages has been considered the most important factor for CNV development (4, 5). NKT cells, as well as inflammatory cytokines, such as IL-1β, IL-6, and TGF-β, were shown to promote CNV, whereas IL-27 suppresses it by modulating VEGF levels (6–9).

IL-17 is a major proinflammatory cytokine linked to the pathogenesis of diverse autoimmune and inflammatory diseases, such as rheumatoid arthritis (RA), psoriasis, inflammatory bowel disease, and uveitic diseases. Of note, IL-17 was shown to be proangiogenic and to induce endothelial cell invasion (10). IL-17 has the potential to upregulate VEGF from RA synoviocytes (11) and to promote the development of microvessel structures in RA, as well as in tumor growth (12, 13). Recently, a subset of effector Th cells, the IL-17–producing T cell (Th17), was implicated in the pathogenesis of various autoimmune diseases, including uveitis, arthritis, multiple sclerosis, psoriasis, and inflammatory bowel disease. In addition, γδT cells, as well as innate lymphoid cells (ILCs), have been implicated as IL-17–producing cells (14). A recent study suggested that C5a promoted IL-22 and IL-17 expression from CD4$^+$ T cells in AMD patients (15). Intriguingly, this study found significantly increased levels of IL-22 and IL-17 in the sera of AMD patients, suggesting possible roles for IL-22 and IL-17 in the inflammation that contributes to CNV and AMD. However, the role of IL-17 and mechanism of IL-17 expression in experimental CNV have not been investigated.

In this study, using gene-disrupted mice and inoculation with Abs, we demonstrated that IL-17 is essential for the development of laser-induced CNV. We identified infiltrated γδT cells, but not Th17 cells, along with Thy-1$^+$ ILCs as the main sources of IL-17 in the laser-treated eye. Furthermore, we found that IL-1β and high-mobility group box 1 (HMGB-1), rather than IL-23, play critical roles in the infiltration of IL-17–producing cells. Moreover, IL-1β, HMGB-1, and γδT cells were shown to be essential for inducing IL-17, and suppression of these cytokines/cells was therapeutic for

*Department of Microbiology and Immunology, Keio University School of Medicine, Shinjuku-ku, Tokyo 160-8582, Japan; †Japan Science and Technology Agency, Core Research for Evolutional Science and Technology, Chiyoda-ku, Tokyo 102-0075, Japan; ‡Department of Ophthalmology, Graduate School of Medical Sciences, Kyushu University, Fukuoka 812-8582, Japan; and §Department of Ophthalmology, Yamaguchi University Graduate School of Medicine, Ube, Yamaguchi 755-8505, Japan

Received for publication September 5, 2012. Accepted for publication December 9, 2012.

This work was supported by special grants-in-aid from the Ministry of Education, Culture, Sports, Science and Technology of Japan; the Program for the Promotion of Fundamental Studies in Health Science of the National Institute of Biomedical Innovation; the SENSIN Medical Research Foundation; the Mochida Memorial Foundation; the Uehara Memorial Foundation; and the Takeda Science Foundation.

Address correspondence and reprint requests to Prof. Akihiko Yoshimura, Department of Microbiology and Immunology, Keio University School of Medicine, 35 Shinanomachi, Shinjuku-ku, Tokyo 160-8582, Japan. E-mail address: yoshimura@a6.keio.jp

Abbreviations used in this article: AMD, age-related macular degeneration; CNV, choroidal neovascularization; DAMP, damage-associated molecular pattern molecule; HMGB-1, high-mobility group box 1; ILC, innate lymphoid cell; iNKT, invariant NKT; KO, knockout; PC, laser photocoagulation; RA, rheumatoid arthritis; RPE, retinal pigment epithelium; VEGF, vascular endothelial growth factor; WT, wild-type.

www.jimmunol.org/cgi/doi/10.4049/jimmunol.1202495

experimental CNV. Our study indicates that IL-17 plays a central role in CNV and could serve as a therapeutic target for AMD.

Materials and Methods

Animals

C57BL/6 (wild-type [WT]) mice, 6–10 wk of age, were purchased from CLEA (Tokyo, Japan) and were kept under specific pathogen–free conditions at Keio University. IL-17 knockout (KO) (16) and IL-23p19 KO (17) mice were described previously. RAG2 KO and TCRγδ KO mice were purchased from The Jackson Laboratory (Bar Harbor, ME). TLR2 and TLR4 KO mice were provided by Dr. S. Akira (Laboratory of Host Defense, Osaka University, Osaka, Japan). All mice were on the C57BL/6 background. All animal experiments were conducted in accordance with the Association for Research in Vision and Ophthalmology Statement for the Use of Animals.

Induction and evaluation of CNV

CNV was induced by laser photocoagulation (PC) and evaluated as described previously (18). Briefly, PC (wavelength = 532 nm, 0.1 s, spot size = 75 μm, power = 200 mW) was performed at four spots around the optic disc of one eye of each mouse. Abs and recombinant proteins were inoculated into the vitreous cavities with a microsyringe immediately after laser treatment. On day 7 after laser treatment, the mice were perfused with 1 ml PBS containing 50 mg/ml fluorescent-labeled dextran (25,000 m.w.; Sigma-Aldrich, St. Louis, MO), and the eyes were removed. The entire retina was carefully dissected from the eyecup and flat-mounted on an aqua-mount with the sclera facing downward and the choroid facing upward. The images were captured using conventional fluorescence microscopy (BZ-8000; Keyence) for CNV area measurement or confocal laser microscopy (LSM510 META; Carl Zeiss) for CNV volume measurement. The hyperfluorescent area and volume corresponding to a photocoagulation spot for each treated eye was evaluated using ImageJ software and subjected to semiquantitative analysis.

Vitreous cavity injection

rIL-17, anti–IL-17 Ab, anti-VEGFA Ab, and rIL-1ra (R&D Systems, Minneapolis, MN) were inoculated into the vitreous cavity using fine, 32-Ga needles (cat. no. 0160832) and 10-μl syringes (cat. no. 80330; both from Hamilton, Reno, NV). The tip of the needle penetrated the sclera, choroid, and retina to reach the vitreous cavity, and a maximum volume of 2 μl/injection was applied per eye. We ensured that the Ag was injected into the vitreous cavity by carefully guiding the tip of the needle under the microscope, through the flattened cornea, which was covered by a glass microscope slide. Inoculating 2 μl solution increased the intraocular pressure sufficiently to seal the retinal incision completely without bleeding or detachment. We considered the total volume of the murine eye to be 10 μl; therefore, 2 μl inoculated Ab solution was diluted five times in vivo. The concentration of each inoculating Ab/recombinant cytokine was determined according to the manufacturer's instructions so as to be sufficient for neutralization or supplementation in vivo.

Real-time RT-PCR

Total RNA was extracted from whole eyes, with the exception of the conjunctiva. Samples from two eyes were pooled to obtain a sufficient amount of mRNA for analysis. The RNA was extracted using Sepasol-RNA I Super G (Nacalai Tesque, Kyoto, Japan), according to the manufacturer's instructions. RNA was reverse transcribed to cDNA with random primers and a high-capacity cDNA reverse transcription kit (both from Applied Biosystems, Carlsbad, CA), in accordance with the manufacturer's instructions. Gene expression was examined using a Bio-Rad (Hercules, CA) iCycler Optical System and SsoFast EvaGreen Supermix. The results were normalized to *HPRT* levels. The primers used were as follows: 5′-CAGCAGCGATCATCCCTCAAAG-3′ and 5′-CAGGACCAGGATCTCTTGCTG-3′ for *IL-17*; 5′-CAGGCAGGCAGTATCACTCA-3′ and 5′-AGGCCACAGGTATTTTGTCG-3′ for *IL-1β*; 5′-ACCTCCACTGCCAGCTGTGTGCTG-TC-3′ and 5′-TCATTTCTGCACTTCTGCATGTAGACTGTCCC-3′ for *RORγt*; 5′-TGAAGAGCTACTGTAATGATCAGTCAAC-3′ and 5′-AGCAAGCTTGCAACCTTAACCA-3′ for *HPRT*; and 5′-CCATTGGTGATGTTGCAAAG-3′ and 5′-CTTTTTCGCTGCATCAGGTT-3′ for *HMGB-1*.

Immunohistochemistry

As reported previously (19), hamster anti-mouse TCRγδ (BD Biosciences, Franklin Lakes, NJ) and rabbit polyclonal anti–HMGB-1 (Abcam, Cambridge, U.K.) were used as primary Abs and incubated at 4°C overnight. Goat anti-rabbit IgG conjugated to Alexa Fluor 488 was used as a secondary Ab and incubated at room temperature for 1 h.

Isolation of ocular-infiltrating cells and flow cytometric analysis

To examine phenotypes, ocular-infiltrating cells were prepared as described previously (5). After PC, the eyes were enucleated, and the posterior segments of two eyes were used for FACS analysis. For intracellular cytokine staining, cells were stimulated for 4.5 h in complete medium with phorbol 12-myristate 13-acetate (50 ng/ml) and ionomycin (500 ng/ml; both from Sigma-Aldrich) in the presence of brefeldin A (eBioscience, San Diego, CA). Surface staining was then performed in the presence of Fc-blocking Abs (2.4G2), followed by intracellular staining for cytokines with a fixation and permeabilization kit (eBioscience), according to the manufacturer's instructions. All Abs were obtained from eBioscience. Data were acquired using a BD FACSAria or BD FACSCanto II and were analyzed with FlowJo software (Tree Star, Ashland, OR).

Transfer of γδT cells or CD4$^+$ T cells into Rag2 *KO mice*

CD3$^+$ T lymphocytes were prepared from the spleens and lymph nodes of WT mice by negative selection using magnetic beads (Miltenyi Biotec, Bergisch Gladbach, Germany) (typically >95% purity) (20). A total of 3×10^5 CD3$^+$CD4$^-$TCRγδ$^+$ cells from WT mice or 1×10^6 CD3$^+$CD4$^+$ TCRγδ$^-$ cells from WT mice, purified through flow cytometry, was injected i.v. into *Rag2* KO mice. Four days after cell transfer, the mice were subjected to laser treatment; 1 wk later, the eyes were enucleated for evaluation of CNV.

In vitro assay

A total of 1×10^5 CD3$^+$CD4$^-$TCRγδ$^+$ T cells was cultured for 48 h with 1 ng/ml plate-bound anti-CD3 Ab (clone 145-2C11) in the presence of 0.1–10 ng/ml rIL-1β (PeproTech, London, U.K.), 1 ng/ml IL-23 (PeproTech), or 1 μg/ml HMGB-1 (Shino-Test, Tokyo, Japan). The amount of secreted IL-17 protein in the supernatants was measured using ELISA (eBioscience), according to the manufacturer's instructions.

Statistical analyses

All data are expressed as mean ± SE and were analyzed using the Dunnett test and the independent-samples t test. The p values < 0.05 were considered statistically significant.

Results

IL-17 promotes choroidal neovascularization after laser treatment

Because a recent report (15) showed a significant increase in IL-17 levels in the sera of AMD patients, we investigated the role of IL-17 in laser-induced CNV in mice. After laser treatment to the eye, expression of *Il17a* mRNA significantly increased from day 3, peaked at day 4, and then gradually decreased (Fig. 1A). To investigate the functional role of IL-17 in ocular neovascularization, *Il17a*-deficient (IL-17 KO) mice were examined. On day 7 after laser treatment, CNV was visualized by the perfusion of fluorescent-labeled dextran, and the green neovascularized areas were measured on choroidal flat mounts. Compared with control mice, IL-17 KO mice exhibited significantly smaller areas of CNV (Fig. 1B). In contrast, areas of CNV were significantly larger in WT mice inoculated with rIL-17 than in untreated WT mice (Fig. 1C). These data indicate that IL-17 promotes CNV development.

We investigated the relationship between IL-17 and VEGF. Unexpectedly, WT and IL-17 KO mice had similar VEGF mRNA levels in their injured eyes (Fig. 1D). Next, we compared the effect of depletion of VEGF and IL-17 on CNV development using Abs. When anti–IL-17 Ab was inoculated into the vitreous cavity, CNV volume was reduced (Fig. 1E, 1F). The suppressive effect of anti–IL-17 Ab on CNV volume and area was similar to that of anti-VEGF

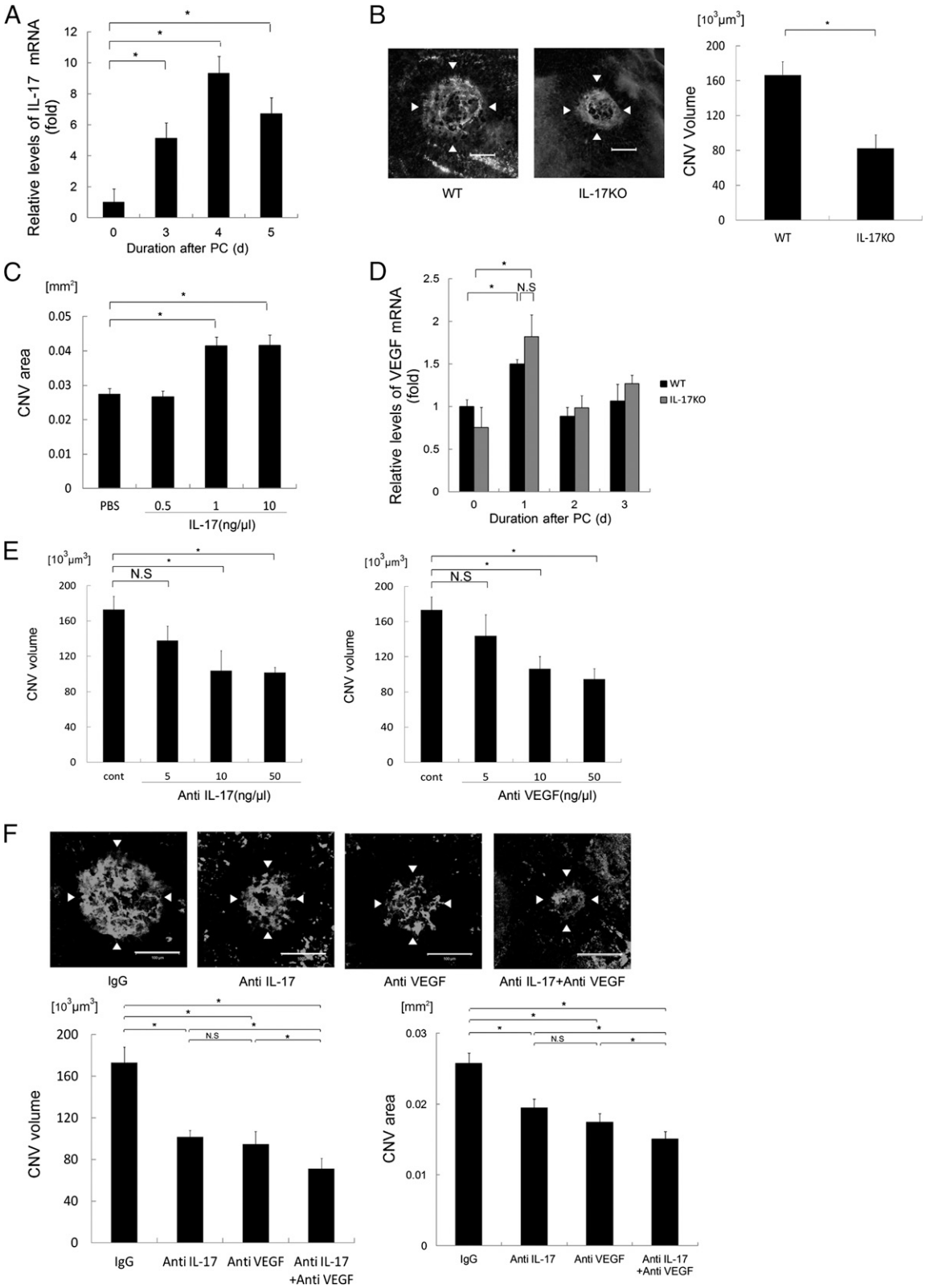

FIGURE 1. Angiogenic activity of IL-17 in CNV. (**A**)Total RNA was extracted from the eyes of WT mice on the indicated days after laser treatment ($n = 3$). *Il17a* mRNA levels were normalized to *HPRT* levels in each sample. (**B**) On day 7 after laser treatment, the sizes of CNV volumes were compared in WT mice and IL-17 KO mice ($n = 10–15$). Representative CNV lesions of choroidal flat mounts are shown. Arrowheads indicate stained CNV tissues. Scale bars, 100 μm. (**C**) rIL-17 (0.5, 1, or 10 ng/μl; 2 μl) was inoculated into the vitreous cavities of WT mice immediately after laser treatment ($n = 10–15$). On day 7 after laser treatment, the sizes of CNV areas were compared among each group. The experiments were repeated three times, with similar results. Data are mean ± SE. $*p < 0.01$. (**D**) *vegf* mRNA levels were compared in laser-treated WT and IL-17 KO mice at several time points ($n = 3$). The experiments were repeated three times, with similar results. Data are mean ± SE. $*p < 0.05$. (**E**) WT mice were inoculated with control IgG (10 ng/μl; 2 μl), anti–IL-17 Ab (2 μl, *left panel*), anti-VEGF Ab (2 μl, *right panel*) into the vitreous cavities immediately after laser treatment ($n = 10–15$). On day 7 after laser treatment, the sizes of CNV volumes were compared (*Figure legend continues*)

Ab (Fig. 1E, 1F). The combination of anti-VEGF and anti-IL-17 Abs was more effective than was the administration of either Ab alone (Fig. 1F). These data indicate that IL-17 has a strong potential for promoting neovascularization in a VEGF-independent manner in experimental CNV.

Although volume measurement by confocal microscopy was more sensitive than area measurement by conventional fluorescent microscopy, essentially similar effects were observed using these two methods (Fig. 1F). Thus, we primarily used area measurement in later experiments because of the convenience of fluorescence microscopy.

Infiltrated γδT cells and ILCs are the main source of IL-17 in the laser-treated eye

IL-17 was shown to be secreted not only from Th17 cells but also from innate immune cells (14), γδT cells (21), and invariant NKT (iNKT) cells (22). Based on these reports, we performed intracellular staining to investigate which cells produce IL-17 in the laser-treated eye. The number of IL-17$^+$ cells increased after laser treatment (Fig. 2A, *upper panels*). Approximately 70% of IL-17$^+$ cells were also CD3$^+$, and most of these IL-17$^+$ cells were γδT cells not Th17 cells (Fig. 2A, *lower panels*). The other 30% of the IL-17$^+$ cells were CD45$^+$ but CD3$^-$ and also Thy-1$^+$ and Lin$^-$ (CD11b, B220, NK1.1, Gr-1), suggesting that ~30% of IL-17–producing cells in choroid regions exhibiting CNV are ILCs (Fig. 2B). These cells were negative for NKp46, CD127, CD122, and CD25, suggesting that these ILCs were not LTi or ILC22 (data not shown). In this fraction, both Sca1$^+$ and Sca1$^-$ cells were included, suggesting a mixture of heterogeneous populations.

Immunohistochemical analysis of retina and RPE/choroid sections revealed that γδT cells infiltrated into laser-injury lesions in the choroid regions (Fig. 2C). Furthermore, IL-17–producing γδT cells were completely absent in the laser-treated eyes of mice lacking RORγt, a master transcription factor for IL-17 transcription (23, 24) (Fig. 2D). These results indicate that infiltrating γδT cells are the main source of IL-17 in the eye after laser treatment. To clarify the importance of infiltrating γδT cells in CNV development, we examined TCRγδ KO mice and found that their *Il17a* mRNA expression levels, as well as their IL-17$^+$ cell counts, were significantly lower than those in WT mice (Fig. 2E, 2F). The areas of CNV after laser treatment were smaller in TCRγδ KO mice than in WT mice (Fig. 2G). Although not statistically significant, administration of Ab against IL-17 always decreased the size of CNV areas in TCRγδ KO mice or Rag2-deficient mice, suggesting a small contribution of IL-17–producing ILCs to CNV formation (Fig. 2G, data not shown for Rag2$^{-/-}$ mice). Adoptive transfer of T lymphocytes into Rag2-deficient (*rag2*KO) mice confirmed that γδT cells, but not conventional CD4$^+$ T cells, were the major producers of IL-17 and that they greatly contributed to ocular neovascularization after laser injury (Fig. 2H). These data suggest that IL-17, as well as IL-17–producing cells, could be therapeutic targets in the treatment of CNV. In addition, targeting the mechanism of IL-17 production in the injured eye could be a useful means of preventing CNV.

IL-1β, but not IL-23, plays a pivotal role in IL-17 induction and laser-induced CNV

Next, we investigated which innate cytokines induce IL-17 from γδT cells, because targeting the mechanism of IL-17 production in the injured eye could be a useful means of preventing CNV. IL-23 was reported to be indispensable in the proliferation of these cells and in their ability to produce IL-17 (25, 26). However, to our surprise, the degree to which CNV areas developed in IL-23p19 KO mice was identical to or only slightly less than that seen in WT mice (Fig. 3A). IL-17$^+$ γδT cells, as well as *Il17a* mRNA, were present in the IL-23p19 KO mice, although IL-17 levels were slightly lower in these mice than in WT mice (Fig. 3B, 3C). These results suggest that IL-23 plays a limited role in IL-17 induction, and there is an IL-23–independent mechanism that stimulates IL-17 production from γδT cells.

Because IL-1β was shown to play a crucial role in inducing IL-17 production in vivo (26), we investigated its role next. IL-1β was shown to be rapidly upregulated in laser-induced CNV (8). We noticed that *Il1b* mRNA levels in the CNV regions were higher in IL-23p19 KO mice than in WT mice (data not shown), suggesting that IL-1β may be more important than IL-23 in the laser-induced CNV model. To test this, we blocked the effect of IL-1β using an IL-1R antagonist (IL-1ra). Consistent with the results of a previous report (8), treatment of mice with IL-1ra reduced the size of the CNV areas in both WT and IL-23p19 KO mice (Fig. 4A). IL-1ra treatment also reduced *Il17a* mRNA levels and the number of IL-17–producing cells in both WT and IL-23p19 KO mice (Fig. 4B, 4C). The number of IL-17–producing cells was not significantly different between WT and IL-23 KO mice, although we always observed some reduction of IL-17$^+$ cells in IL-23 KO mice. Furthermore, IL-1β potently induced IL-17 production from γδT cells more efficiently than did IL-23 in vitro (Fig. 4D). These data indicate that IL-1β, rather than IL-23, plays more important roles in the induction of IL-17–producing γδT cells, as well as laser-induced CNV formation in the eye.

HMGB-1 as an inducer of IL-1β from macrophages and IL-17 from γδT cells

Given that IL-1β was shown to be mostly produced from macrophages (27), we investigated the endogenous TLR ligand that can induce macrophages to produce IL-1β. We confirmed that CNV areas were smaller in TLR2- and TLR4-deficient mice than in WT mice (Fig. 5A). HMGB-1 was reported to be involved in Th17 development in an experimental autoimmune encephalomyelitis model (28) and to play important roles in alkaline-induced corneal neovascularization through TLR4 (29). We observed that HMGB-1 also upregulated IL-17 secretion from γδT cells in collaboration with IL-1β (Fig. 4D). Thus, we investigated the role of HMGB-1 in IL-17 induction in our laser-induced CNV model. HMGB-1 proteins are usually contained in the nucleus but can be released into the extracellular milieu as the result of injury or other forms of stress (30). In the retina, degenerated photoreceptors exhibit augmented HMGB-1 expression after retinal detachment (31). HMGB-1 mRNA expression was increased soon after laser exposure (Fig. 5B). HMGB-1 ex-

among the four groups. The experiments were repeated three times, with similar results. Data are mean ± SE. *$p < 0.01$. (**F**) WT mice were inoculated with control IgG (10 ng/μl, 2 μl), anti–IL-17 Ab (10 ng/μl; 2 μl), anti-VEGF Ab (10 ng/μl; 2 μl), or the combination of anti–IL-17 (20 ng/μl; 1 μl) and anti-VEGF Abs (20 ng/μl; 1 μl) into the vitreous cavities immediately after laser treatment (n = 10–15). Representative CNV lesions of choroidal flat mounts of each group are shown on day 7 after laser treatment. Arrowheads indicate stained CNV tissues. Scale bars, 100 μm. The sizes of CNV volumes and areas were compared among four groups. The experiments were repeated three times, with similar results. Data are mean ± SE. *$p < 0.01$.

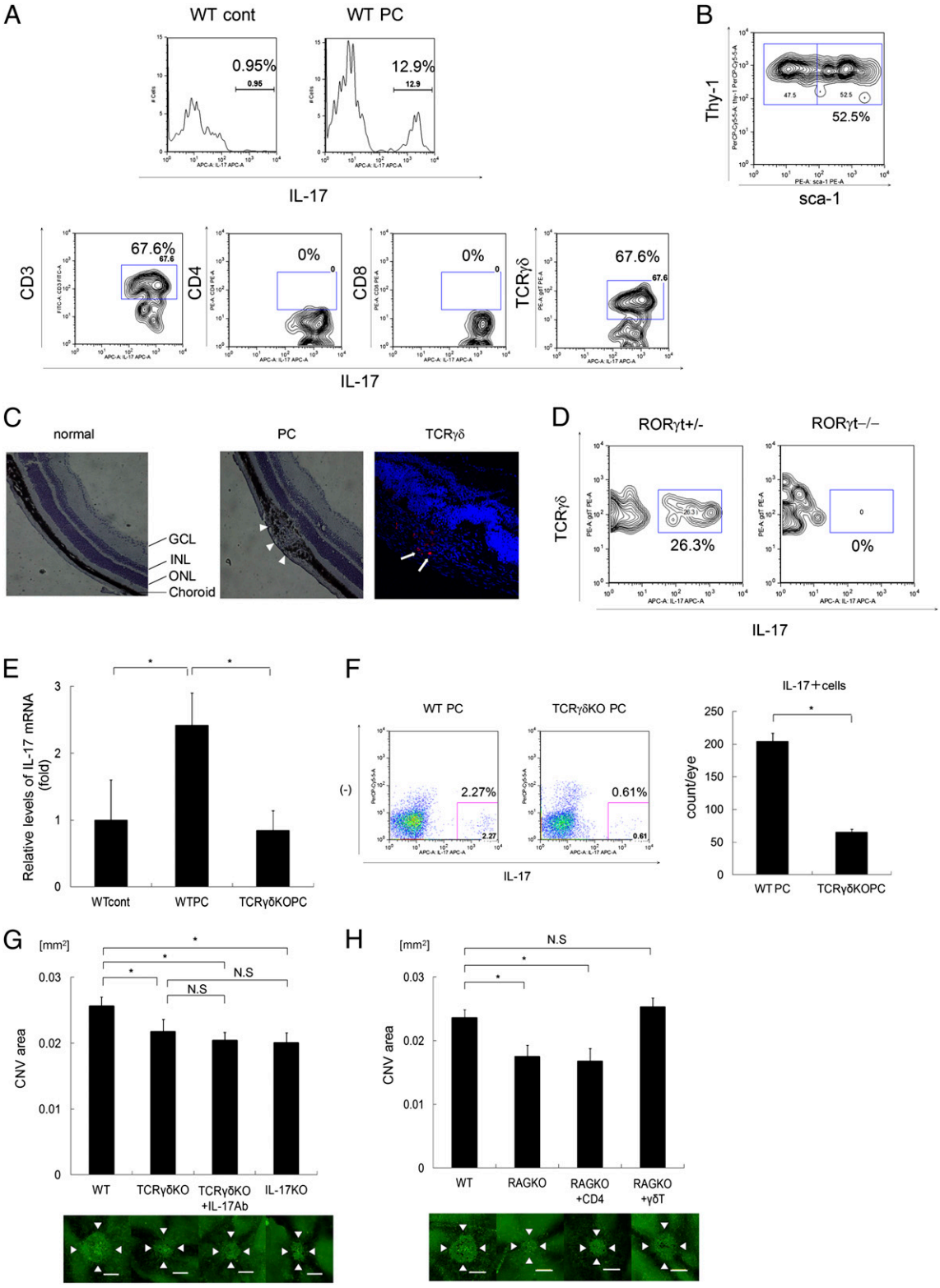

FIGURE 2. The source of IL-17 in the laser-treated eye. (**A**) Ocular-infiltrating cells were analyzed 4 d after laser treatment. The production of IL-17A in cells was examined by intracellular staining. WT laser-treated eye samples gated for CD45$^+$ cells (*upper panels*). Samples gated for IL-17A$^+$ cells (*lower panels*). One representative experiment of three independent experiments is shown. (**B**) The IL-17A$^+$ cell population in TCRγδ KO mice was analyzed for Thy-1 and Sca-1 expression levels by flow cytometry. (**C**) Immunohistochemical analysis of retina and RPE/choroid sections on day 4 after laser treatment. H&E staining of the retina and RPE/choroid sections of control and laser-treated mice (*left* and *middle panel*, respectively). The retina and RPE/choroid sections were stained with anti-TCRγδ (red) (arrow in *right panel*). Representative images are shown. Arrowheads denote laser photocoagulated site. Original magnification ×10. (**D**) Intracellular staining data for IL-17A in laser-treated *Rorγt*$^{+/gfp}$ mice and *Rorγt*$^{gfp/gfp}$ mice on day 4 after laser treatment. The panels show the results of gating for TCRγδ$^+$ cells in laser-treated eye samples from each mouse. (**E**) Total RNA was extracted from the eyes of WT mice and TCRγδ KO mice on day 4 after laser treatment ($n = 3$). *Il17a* mRNA levels were normalized to *HPRT* levels in each sample. *$p < 0.01$. (**F**) Intracellular staining data on IL-17A in laser-treated WT mice and TCRγδ KO mice on day 4 after laser treatment ($n = 2$). The bar graph represents the fraction of the IL-17A$^+$ cell populations. The (*Figure legend continues*)

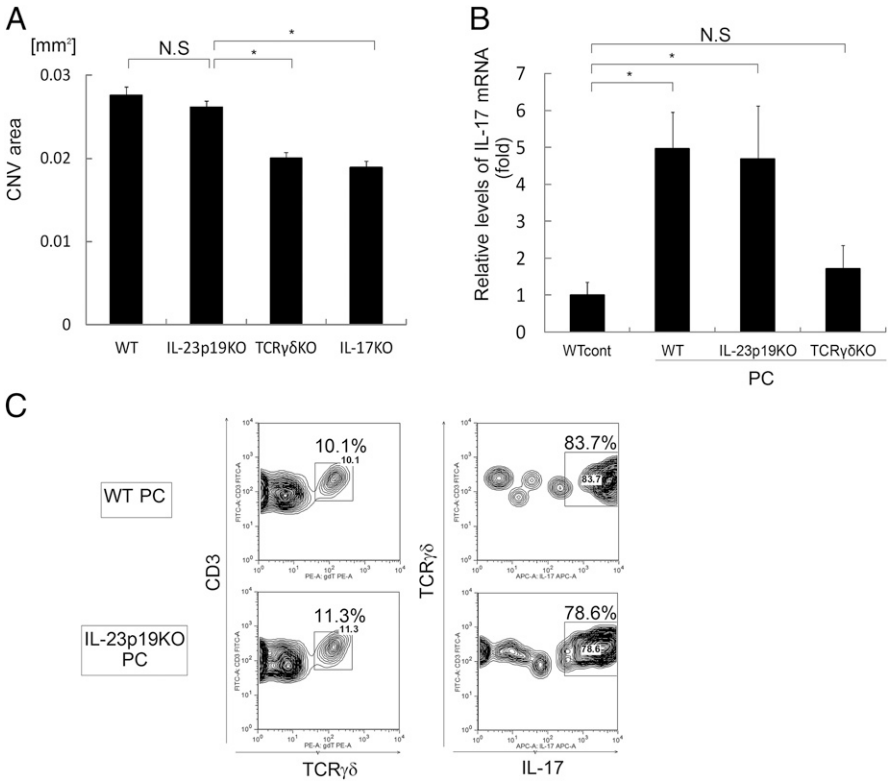

FIGURE 3. IL-17 induction and CNV promotion were independent of IL-23. (**A**) On day 4 after laser treatment, the sizes of CNV areas were compared among four groups: WT mice, IL-23p19 KO mice, TCRγδ KO mice, and IL-17 KO mice (n = 10–15). The experiment was repeated three times with similar results. Data are mean ± SE. *$p <$ 0.01. (**B**) The expression levels of *IL17a* mRNA in laser-treated eyes from WT mice, IL-23p19 KO mice, and TCRγδ KO mice were monitored using real-time PCR on day 4 after laser treatment, and the data were normalized to *HPRT* levels (n = 3). *$p <$ 0.01. (**C**) Ocular-infiltrating cells of WT mice (*upper panels*) and IL-23p19 KO mice (*lower panels*) were analyzed on day 4 after laser treatment (n = 2). Results of gating for CD3 (*left panels*) and TCRγδ$^+$ (*right panels*) cells are shown for each eye sample. The production of IL-17A in cells was examined by intracellular staining (*right panels*). One representative experiment of three independent experiments is shown.

pression was induced in RPE and photoreceptor cells at the laser-injured choroid (Fig. 5C). An Ab against HMGB-1 reduced the size of CNV areas (Fig. 5D), as well as the rate of infiltration of IL-17$^+$ γδT cells (Fig. 5E). HMGB-1 blockade reduced IL-1β production (Fig. 5F). Furthermore, rHMGB-1 induced IL-1β in a RAW macrophage cell line (Fig. 5G). Taken together, these findings indicate that injured photoreceptor cells express damage-associated molecular pattern molecules (DAMPs), including HMGB-1, which results in the induction of IL-1β, which, in turn, promotes IL-17 secretion from γδT cells. HMGB-1 may also directly stimulate IL-17 production from γδT cells in collaboration with IL-1β, because γδT cells were reported to respond to TLR ligands (32). As expected, rHMGB-1 upregulated IL-17 levels in γδT cells in vitro in the presence of IL-1β (Fig. 4D). Thus, reducing patients' levels of IL-1β or HMGB-1, similar to a reduction in IL-17 level, might be an effective strategy for the prevention of CNV (Fig. 6).

Discussion

The laser-induced CNV mouse model is well established for investigating ocular angiogenesis (33). As with human AMD, suppression of angiogenesis by an anti-VEGF Ab is therapeutic for laser-induced CNV (18). This model system is eminently useful for identifying promising therapeutic targets for human AMD. For example, Takeda et al. (34) identified CCR3, a receptor found on eosinophils and mast cells, which are immune mediators of allergic inflammation, as an essential chemokine receptor for the growth of choroidal vessels in CNV. They demonstrated that blockade of intraocular CCR3 with neutralizing Abs or receptor antagonists significantly decreased the generation of abnormal blood vessels in the choroid after laser injury in a CNV mouse model. CCR3 was shown to be expressed in the endothelial cells lining the abnormal blood vessels of CNV in wet AMD patients, suggesting that the eotaxin–CCR3 axis is functional in human disease.

In the current study, we demonstrated that IL-17 plays an important role in promoting ocular neovascularization, and γδT cells, as well as a small fraction of ILCs, are the main sources of IL-17 in this laser-injury model. A recent study showed that IL-17 and IL-22 are elevated in the sera of AMD patients and that C5a promotes the production of these cytokines from human CD4$^+$ T cells (15). In our experimental CNV mouse model, γδT cells, rather than Th17 cells, were the major (~70%) source of IL-17. Another recent study showed that γδT cells express a C5a receptor and promote IL-17 production by C5a stimulation (35). However, because laser-induced CNV is an acute-injury model, the role of C5a in this system remains to be clarified.

Interestingly, VEGF levels were not affected by IL-17 deficiency (Fig. 1D). This suggests that IL-17 functions as a proangiogenic factor in a VEGF-independent manner, and anti–IL-17 therapy could be useful for patients resistant to anti-VEGF therapy. Moreover, a combined therapy aimed at these two

experiments were repeated three times with similar results. Data are mean ± SE. *$p < 0.01$. (**G**) On day 7 after laser treatment, the sizes of CNV areas were evaluated and compared among WT mice, IL-17 KO mice, TCRγδ KO mice, and TCRγδ KO mice with Ab to IL-17 (10 ng/μl; 2 μl) inoculation into the vitreous cavities immediately after laser treatment (n = 10–15). Data are mean ± SE. The experiment was repeated three times with similar results. Arrowheads indicate stained CNV tissues. Scale bars, 100μm. *$p < 0.01$. (**H**) A total of 3×10^5 CD3$^+$CD4$^-$TCRγδ$^+$ cells from WT mice or 1×10^6 CD3$^+$CD4$^+$TCRγδ$^-$ cells from WT mice, purified by means of flow cytometry, were injected i.v. into *Rag2* KO mice. At 4 d after cell transfer, the mice were subjected to laser treatment. On day 7 after laser treatment, eyes were enucleated for evaluation of CNV. Arrowheads indicate stained CNV tissues. Scale bars, 100μm. *$p < 0.01$. GCL, Ganglion cell layer; INL, inner nuclear layer; ONL, outer nuclear layer.

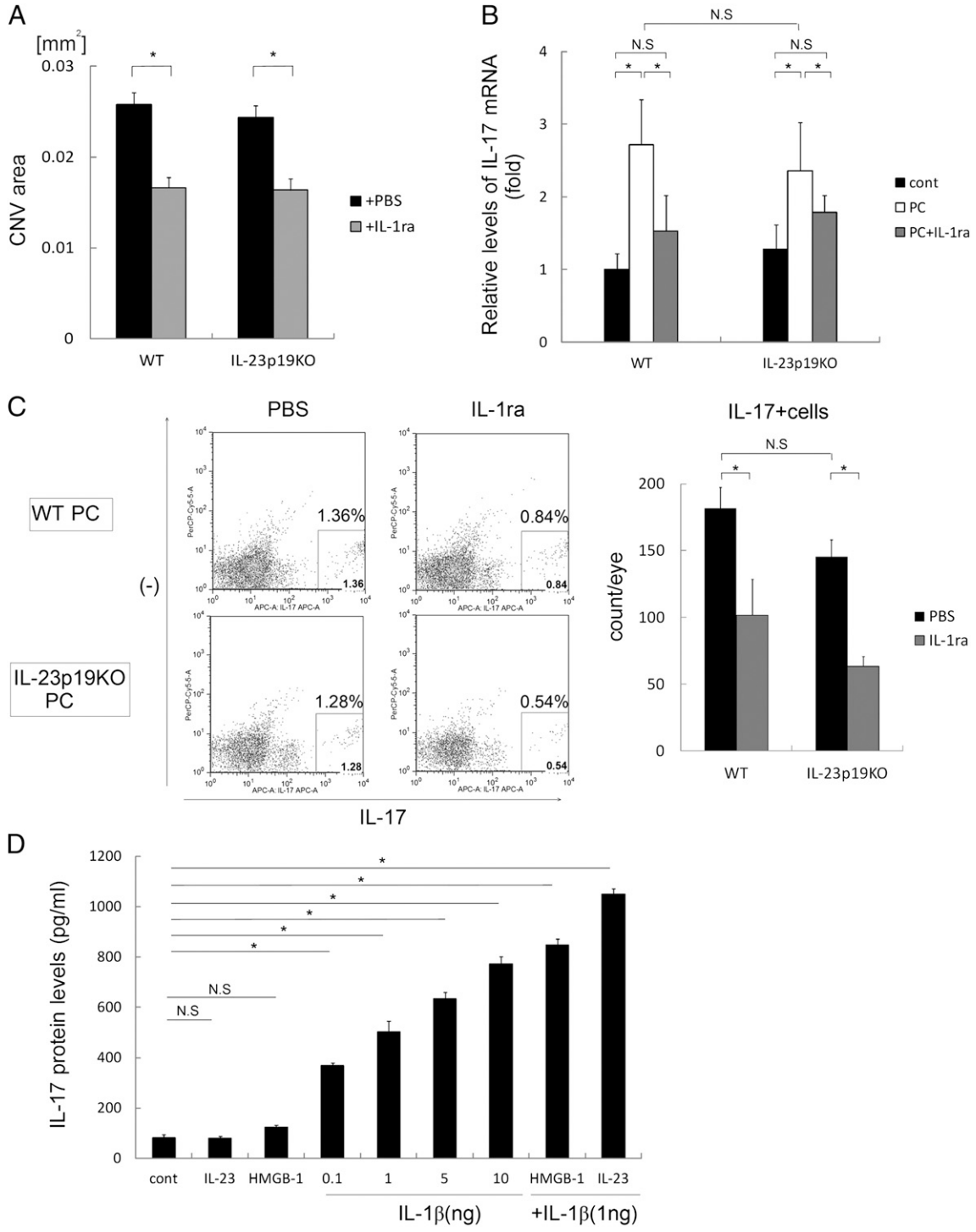

FIGURE 4. Suppression of IL-17 induction and CNV by blockade of IL-1β. (**A**–**C**) WT mice and IL-23p19 KO mice were subjected to laser treatment and inoculated with IL-1ra (1 ng/μl; 2 μl) or PBS (2 μl) into the vitreous cavities immediately after laser treatment. (A) The sizes of CNV areas were compared in WT mice and IL-23p19 KO mice inoculated with IL-1ra or PBS on day 7 (n = 10–15). (B) The expression levels of *Il17a* mRNA in laser-treated eyes from WT mice and IL-23p19 KO mice were monitored on day 4 by real-time PCR, and the data were normalized to HPRT expression (n = 3). Data are mean ± SE. *$p < 0.01$. (C) Intracellular staining data for IL-17A in laser-treated WT and IL-23p19 KO mice on day 4 after laser treatment (n = 2). The bar graph represents the fraction of the IL-17A$^+$ cell populations. The experiments were repeated three times with similar results. Data are mean ± SE. *$p < 0.01$. (**D**) A total of 1×10^5 γδT purified cells from WT mice was cultured with anti-CD3 in the presence of IL-1β, with or without IL-23 and HMGB-1. After 48 h, the amount of secreted IL-17 protein in the supernatants was measured using ELISA. Data are mean ± SE. *$p < 0.01$.

cytokines may be more powerful than a single-treatment approach. Although there are a number of reports suggesting that IL-17 promotes angiogenesis by directly stimulating endothelial cells, the precise mechanism of angiogenesis by IL-17 is not clear. Other reports indicate that VEGF is induced by IL-17 (11). Thus, we could not completely rule out the possibility that VEGF induced by IL-17 participates in CNV formation in WT animals (Fig. 6).

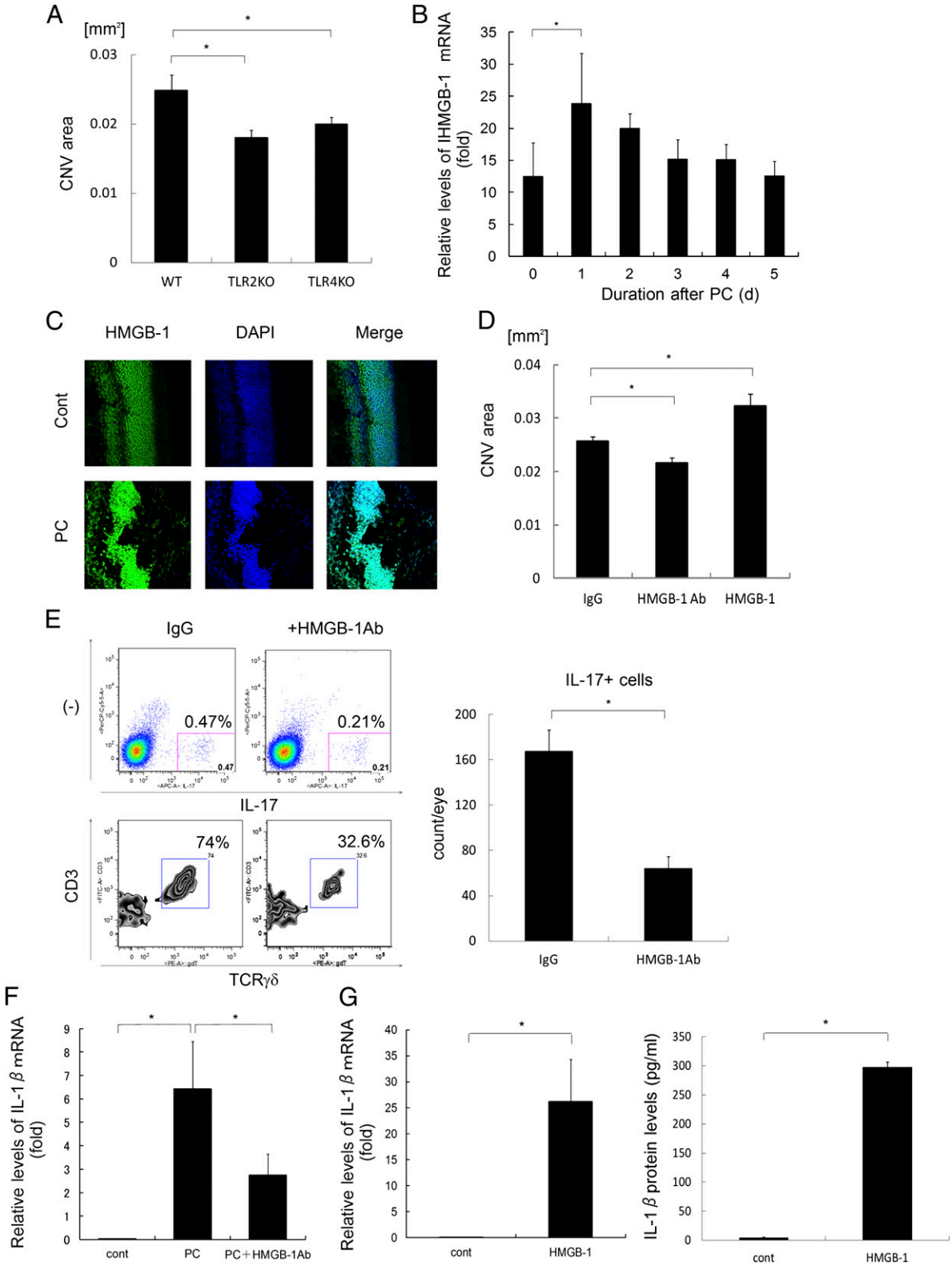

FIGURE 5. Suppression of IL-17 and IL-1β induction by blockade of HMGB-1. (**A**) On day 7 after laser treatment, the sizes of CNV areas were compared among WT, TLR2, and TLR4 KO mice (n = 10–12). The experiments were repeated three times with similar results. Data are mean ± SE. *$p < 0.01$. (**B**) Total RNA was extracted from the eyes of WT mice on the indicated days after laser treatment (n = 3). *HMGB-1* mRNA levels were normalized to HPRT levels in each sample. Data are mean ± SE. *$p < 0.05$. (**C**) Immunohistochemical analysis of normal retina and RPE/choroid sections (*upper panels*) or retina and RPE/choroid sections 4 d after laser treatment (*lower panels*). The retina and RPE/choroid sections were double stained with anti–HMGB-1 (green) and DAPI (blue). Original magnification ×10. (**D**) On day 7 after laser treatment, the sizes of the CNV areas were compared among WT mice inoculated with control IgG, Ab to HMGB-1, or HMGB-1 into the vitreous cavities immediately after laser treatment (n = 10–15). Data are mean ± SE. *$p < 0.01$. (**E**) Intracellular staining data for IL-17A in laser-treated WT mice on day 4 with or without Ab to HMGB-1 inoculation into the vitreous cavities immediately after laser treatment (n = 2) (*upper panels*). Results of gating for IL-17A$^+$ cells (*lower panels*). The bar graph represents the fraction of the IL-17A$^+$ cell populations. The experiments were repeated (*Figure legend continues*)

In addition to γδT cells, we found that 30% of IL-17 came from $CD3^-Thy1^+$ ILCs. In this fraction, both $Sca1^+$ and $Sca1^-$ cells were included; therefore, a mixture of heterogeneous populations is likely. However, IL-17 production was completely dependent on RORγt. Because IL-17–producing ILCs are reported as being mostly present in the gut (36), the origin of $IL\text{-}17^+$ ILCs in the eye is an intriguing subject. We showed that iNKT cells also play a role in CNV angiogenesis (6), but we could exclude the possibility that $IL\text{-}17^+$ ILCs were iNKT cells because those cells were $CD3^-$.

Another important feature of IL-17 production in the eye is the need for IL-23. IL-23 was reported to play critical roles in IL-17 production from conventional Th17 and γδT cells (26). For example, IL-17 production from Th17 cells and γδT cells infiltrated into the brain was completely dependent on IL-23 in an experimental autoimmune encephalomyelitis model and a brain ischemia model, respectively (17, 21). IL-23 was shown to be a potent inducer of inflammation in autoimmune diseases, RA, psoriasis, encephalomyelitis, and inflammatory bowel diseases. However, in our current study, we demonstrated that γδT cells can produce IL-17 without IL-23 (Fig. 3). With regard to Th17 cells, TGF-β plus IL-6 was shown to be necessary for early development of Th17 in vitro, and IL-23 is not necessary for early Th17 cell development in vitro, but it appears to be required for pathogenic features of Th17 cells. Izcue et al. (37) reported that TGF-β, rather than IL-23, was essential for Th17 development in vivo. However, it was shown that IL-23 is the most potent inducer of IL-17 from γδT cells. We examined other reported IL-17–inducing factors, including bacterial TLR ligands, as well as IL-6, and found that only IL-1β can act as a substitute for IL-23 in inducing IL-17 secretion from γδT cells (Fig. 4). In AMD patients, it was reported that accumulated macrophages in CNV areas and RPE cells secrete IL-1β (27). In mouse models, macrophages also infiltrate the eye (5), and IL-1β expression increases soon after laser treatment (8). Thus, we suspected that IL-1β is an essential factor in the induction of IL-17 from γδT cells, but we could not rule out other factors that stimulate TLRs. For example, we reported that *Chlamydia pneumonia* infection enhances CNV via TLR2 (38).

Because the laser CNV model is dependent on TLR2/4, we suspected that certain TLR ligands might stimulate IL-1β production from macrophages. However, no bacterial infection was evident in our laser-induced models; thus, endogenous DAMPs could be candidates. HMGB-1 protein, heat shock proteins, β-amyloid, and others were reported to be endogenous ligands for TLR and to function as DAMPs (39, 40). A recent study suggests that drusen components activate NLRP3, which induces IL-18, although drusen alone does not seem to activate TLRs (41). We investigated HMGB-1 because rHMGB-1, but not other recombinant proteins, including peroxiredoxins (42), potently induces IL-1β from macrophage-like cells. Secretion of IL-1β requires inflammasome activation, as well as TLR stimulation, and HMGB-1 seems to be able to activate both pathways simultaneously. The mechanism of inflammasome activation by HMGB-1 remains to be clarified. Our data indicated the possibility that HMGB-1 proteins play

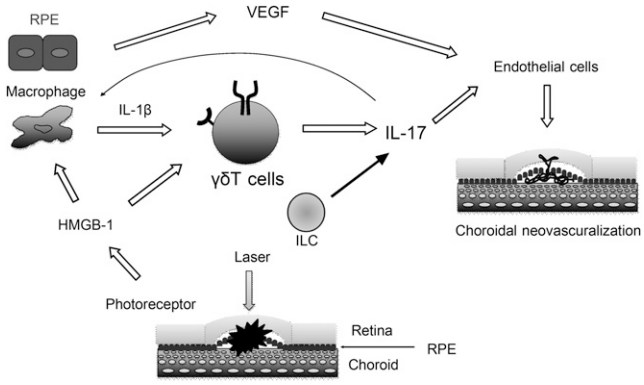

FIGURE 6. Schematic model for the promotion of CNV by IL-17, IL-1β, and HMGB-1. Macrophages are recruited into the injured choroid area and produce IL-1β in response to HMGB-1 stimulation. Then IL-1β induces IL-17 expression from infiltrated γδT cells. HMGB-1 also promotes IL-17 expression from γδT cells in combination with IL-1β. IL-17 functions as an angiogenic factor together with VEGF on endothelial cells.

specific roles at different phases after laser injury. HMGB-1 mRNA levels increased rapidly after laser injury (Fig. 5B). Thus, early HMGB-1 may induce IL-1β from macrophages on day 1, which is consistent with the time course of IL-1β mRNA expression. We also noticed maintained HMGB-1 protein expression in the laser-injured choroid on day 4 (Fig. 5C). We showed that HMGB-1 stimulated IL-17 production in combination with IL-1β from γδT cells. Thus, HMGB-1 protein may enhance IL-17 production from infiltrated γδT cells in a late phase after laser injury.

Apparently, IL-1β is proangiogenic, whereas Doyle et al. (41) showed that IL-18 is antiangiogenic, indicating that IL-1β and IL-18 have opposite functions in CNV formation. Doyle et al. (41) reported that LPS and the complement factor C1Q induced IL-1β at higher levels than IL-18 in vitro, and IL-1β mRNA expression was elevated from a few hours after laser stimulation in the laser-induced CNV model (8). We suspect that, in the early phase of injury, CNV is promoted by the NLRP3–IL-1β pathway, which is activated by strong DAMPs like HMGB-1, whereas, in a late phase, CNV is suppressed by the NLRP3–IL-18 pathway, which is activated by unknown DAMPs to promote tissue repair and remodeling or to maintain the choroidal homeostasis. Because little is known about the induction mechanisms of IL-1β and IL-18, the significance of these two related cytokines in CNV formation remains to be investigated.

The elevated IL-17 levels in the sera (15) suggest that increasing levels of IL-17 in the eye may be involved in the pathogenesis of AMD. Because humanized anti–IL-17 Ab is now in phase II trials for RA and psoriasis, anti–IL-17 therapy may become easily and rapidly applicable for AMD patients. We also expect that the suppression of innate cell activators, such as IL-1β and HMGB-1, could be preventive against the development of human AMD.

three times with similar results. Data are mean ± SE. $*p < 0.01$. (**F**) Total RNA was extracted from the eyes of WT mice, with or without Ab to HMGB-1 inoculation into the vitreous cavities immediately after laser treatment, on day 1 after laser treatment ($n = 3$). *Il1b* mRNA levels were normalized to *HPRT* levels in each sample. $*p < 0.01$. (**G**) RAW cells (2×10^5) were treated or not with 1 μM rHMGB-1 for 24 h. The expression levels of *Il1b* mRNA were monitored using real-time PCR, and the data were normalized to HPRT levels ($n = 3$). IL-1β protein levels in the culture supernatant were determined by ELISA. $*p < 0.01$.

Acknowledgments

We thank Dr. Y. Iwakura (Research Institute for Biomedical Sciences, Tokyo University of Science, Chiba, Japan) for IL-17 KO mice, Dr. D. Cua (Schering-Plough Biopharma, DNAX Discovery Research, Palo Alto, CA) for IL-23 KO mice, and Dr. S. Akira (Laboratory of Host Defense, Osaka University) for TLR2/4 KO mice.

Disclosures

The authors have no financial conflicts of interest.

References

1. Lim, L. S., P. Mitchell, J. M. Seddon, F. G. Holz, and T. Y. Wong. 2012. Age-related macular degeneration. *Lancet* 379: 1728–1738.
2. Tuo, J., S. Grob, K. Zhang, and C. C. Chan. 2012. Genetics of immunological and inflammatory components in age-related macular degeneration. *Ocul. Immunol. Inflamm.* 20: 27–36.
3. Telander, D. G. 2011. Inflammation and age-related macular degeneration (AMD). *Semin. Ophthalmol.* 26: 192–197.
4. Grossniklaus, H. E., J. X. Ling, T. M. Wallace, S. Dithmar, D. H. Lawson, C. Cohen, V. M. Elner, S. G. Elner, and P. Sternberg, Jr. 2002. Macrophage and retinal pigment epithelium expression of angiogenic cytokines in choroidal neovascularization. *Mol. Vis.* 8: 119–126.
5. Tsutsumi, C., K. H. Sonoda, K. Egashira, H. Qiao, T. Hisatomi, S. Nakao, M. Ishibashi, I. F. Charo, T. Sakamoto, T. Murata, and T. Ishibashi. 2003. The critical role of ocular-infiltrating macrophages in the development of choroidal neovascularization. *J. Leukoc. Biol.* 74: 25–32.
6. Hijioka, K., K. H. Sonoda, C. Tsutsumi-Miyahara, T. Fujimoto, Y. Oshima, M. Taniguchi, and T. Ishibashi. 2008. Investigation of the role of CD1d-restricted invariant NKT cells in experimental choroidal neovascularization. *Biochem. Biophys. Res. Commun.* 374: 38–43.
7. Izumi-Nagai, K., N. Nagai, Y. Ozawa, M. Mihara, Y. Ohsugi, T. Kurihara, T. Koto, S. Satofuka, M. Inoue, K. Tsubota, et al. 2007. Interleukin-6 receptor-mediated activation of signal transducer and activator of transcription-3 (STAT3) promotes choroidal neovascularization. *Am. J. Pathol.* 170: 2149–2158.
8. Lavalette, S., W. Raoul, M. Houssier, S. Camelo, O. Levy, B. Calippe, L. Jonet, F. Behar-Cohen, S. Chemtob, X. Guillonneau, et al. 2011. Interleukin-1β inhibition prevents choroidal neovascularization and does not exacerbate photoreceptor degeneration. *Am. J. Pathol.* 178: 2416–2423.
9. Hasegawa, E., Y. Oshima, A. Takeda, K. Saeki, H. Yoshida, K. H. Sonoda, and T. Ishibashi. 2012. IL-27 inhibits pathophysiological intraocular neovascularization due to laser burn. *J. Leukoc. Biol.* 91: 267–273.
10. Moran, E. M., M. Connolly, W. Gao, J. McCormick, U. Fearon, and D. J. Veale. 2011. Interleukin-17A induction of angiogenesis, cell migration, and cytoskeletal rearrangement. *Arthritis Rheum.* 63: 3263–3273.
11. Ryu, S., J. H. Lee, and S. I. Kim. 2006. IL-17 increased the production of vascular endothelial growth factor in rheumatoid arthritis synoviocytes. *Clin. Rheumatol.* 25: 16–20.
12. Pickens, S. R., M. V. Volin, A. M. Mandelin, II, J. K. Kolls, R. M. Pope, and S. Shahrara. 2010. IL-17 contributes to angiogenesis in rheumatoid arthritis. *J. Immunol.* 184: 3233–3241.
13. Numasaki, M., J. Fukushi, M. Ono, S. K. Narula, P. J. Zavodny, T. Kudo, P. D. Robbins, H. Tahara, and M. T. Lotze. 2003. Interleukin-17 promotes angiogenesis and tumor growth. *Blood* 101: 2620–2627.
14. Cua, D. J., and C. M. Tato. 2010. Innate IL-17-producing cells: the sentinels of the immune system. *Nat. Rev. Immunol.* 10: 479–489.
15. Liu, B., L. Wei, C. Meyerle, J. Tuo, H. N. Sen, Z. Li, S. Chakrabarty, E. Agron, C. C. Chan, M. L. Klein, et al. 2011. Complement component C5a promotes expression of IL-22 and IL-17 from human T cells and its implication in age-related macular degeneration. *J. Transl. Med.* 9: 1–12.
16. Nakae, S., Y. Komiyama, A. Nambu, K. Sudo, M. Iwase, I. Homma, K. Sekikawa, M. Asano, and Y. Iwakura. 2002. Antigen-specific T cell sensitization is impaired in IL-17-deficient mice, causing suppression of allergic cellular and humoral responses. *Immunity* 17: 375–387.
17. Cua, D. J., J. Sherlock, Y. Chen, C. A. Murphy, B. Joyce, B. Seymour, L. Lucian, W. To, S. Kwan, T. Churakova, et al. 2003. Interleukin-23 rather than interleukin-12 is the critical cytokine for autoimmune inflammation of the brain. *Nature* 421: 744–748.
18. Krzystolik, M. G., M. A. Afshari, A. P. Adamis, J. Gaudreault, E. S. Gragoudas, N. A. Michaud, W. Li, E. Connolly, C. A. O'Neill, and J. W. Miller. 2002. Prevention of experimental choroidal neovascularization with intravitreal anti-vascular endothelial growth factor antibody fragment. *Arch. Ophthalmol.* 120: 338–346.
19. Oshima, Y., S. Oshima, H. Nambu, S. Kachi, K. Takahashi, N. Umeda, J. Shen, A. Dong, R. S. Apte, E. Duh, et al. 2005. Different effects of angiopoietin-2 in different vascular beds: new vessels are most sensitive. *FASEB J.* 19: 963–965.
20. Tanaka, K., K. Ichiyama, M. Hashimoto, H. Yoshida, T. Takimoto, G. Takaesu, T. Torisu, T. Hanada, H. Yasukawa, S. Fukuyama, et al. 2008. Loss of suppressor of cytokine signaling 1 in helper T cells leads to defective Th17 differentiation by enhancing antagonistic effects of IFN-gamma on STAT3 and Smads. *J. Immunol.* 180: 3746–3756.
21. Shichita, T., Y. Sugiyama, H. Ooboshi, H. Sugimori, R. Nakagawa, I. Takada, T. Iwaki, Y. Okada, M. Iida, D. J. Cua, et al. 2009. Pivotal role of cerebral interleukin-17-producing gammadeltaT cells in the delayed phase of ischemic brain injury. *Nat. Med.* 15: 946–950.
22. Michel, M. L., D. Mendes-da-Cruz, A. C. Keller, M. Lochner, E. Schneider, M. Dy, G. Eberl, and M. C. Leite-de-Moraes. 2008. Critical role of ROR-γt in a new thymic pathway leading to IL-17-producing invariant NKT cell differentiation. *Proc. Natl. Acad. Sci. USA* 105: 19845–19850.
23. Ivanov, I. I., B. S. McKenzie, L. Zhou, C. E. Tadokoro, A. Lepelley, J. J. Lafaille, D. J. Cua, and D. R. Littman. 2006. The orphan nuclear receptor RORgammat directs the differentiation program of proinflammatory IL-17+ T helper cells. *Cell* 126: 1121–1133.
24. Ichiyama, K., H. Yoshida, Y. Wakabayashi, T. Chinen, K. Saeki, M. Nakaya, G. Takaesu, S. Hori, A. Yoshimura, and T. Kobayashi. 2008. Foxp3 inhibits RORgammat-mediated IL-17A mRNA transcription through direct interaction with RORgammat. *J. Biol. Chem.* 283: 17003–17008.
25. Aggarwal, S., N. Ghilardi, M. H. Xie, F. J. de Sauvage, and A. L. Gurney. 2003. Interleukin-23 promotes a distinct CD4 T cell activation state characterized by the production of interleukin-17. *J. Biol. Chem.* 278: 1910–1914.
26. Sutton, C. E., S. J. Lalor, C. M. Sweeney, C. F. Brereton, E. C. Lavelle, and K. H. Mills. 2009. Interleukin-1 and IL-23 induce innate IL-17 production from gammadelta T cells, amplifying Th17 responses and autoimmunity. *Immunity* 31: 331–341.
27. Wang, J., K. Ohno-Matsui, T. Yoshida, N. Shimada, S. Ichinose, T. Sato, M. Mochizuki, and I. Morita. 2009. Amyloid-beta up-regulates complement factor B in retinal pigment epithelial cells through cytokines released from recruited macrophages/microglia: Another mechanism of complement activation in age-related macular degeneration. *J. Cell. Physiol.* 220: 119–128.
28. Su, Z., C. Sun, C. Zhou, Y. Liu, H. Zhu, S. Sandoghchian, D. Zheng, T. Peng, Y. Zhang, Z. Jiao, et al. 2011. HMGB1 blockade attenuates experimental autoimmune myocarditis and suppresses Th17-cell expansion. *Eur. J. Immunol.* 41: 3586–3595.
29. Lin, Q., X. P. Yang, D. Fang, X. Ren, H. Zhou, J. Fang, X. Liu, S. Zhou, F. Wen, X. Yao, et al. 2011. High-mobility group box-1 mediates toll-like receptor 4-dependent angiogenesis. *Arterioscler. Thromb. Vasc. Biol.* 31: 1024–1032.
30. Degryse, B., T. Bonaldi, P. Scaffidi, S. Müller, M. Resnati, F. Sanvito, G. Arrigoni, and M. E. Bianchi. 2001. The high mobility group (HMG) boxes of the nuclear protein HMG1 induce chemotaxis and cytoskeleton reorganization in rat smooth muscle cells. *J. Cell Biol.* 152: 1197–1206.
31. Arimura, N., Y. Ki-i, T. Hashiguchi, K. Kawahara, K. K. Biswas, M. Nakamura, Y. Sonoda, K. Yamakiri, A. Okubo, T. Sakamoto, and I. Maruyama. 2009. Intraocular expression and release of high-mobility group box 1 protein in retinal detachment. *Lab. Invest.* 89: 278–289.
32. Martin, B., K. Hirota, D. J. Cua, B. Stockinger, and M. Veldhoen. 2009. Interleukin-17-producing gammadelta T cells selectively expand in response to pathogen products and environmental signals. *Immunity* 31: 321–330.
33. Ryan, S. J. 1979. The development of an experimental model of subretinal neovascularization in disciform macular degeneration. *Trans. Am. Ophthalmol. Soc.* 77: 707–745.
34. Takeda, A., J. Z. Baffi, M. E. Kleinman, W. G. Cho, M. Nozaki, K. Yamada, H. Kaneko, R. J. Albuquerque, S. Dridi, K. Saito, et al. 2009. CCR3 is a target for age-related macular degeneration diagnosis and therapy. *Nature* 460: 225–230.
35. Han, G., S. Geng, Y. Li, G. Chen, R. Wang, X. Li, Y. Ma, B. Shen, and Y. Li. 2011. γδT-cell function in sepsis is modulated by C5a receptor signalling. *Immunology* 133: 340–349.
36. Buonocore, S., P. P. Ahern, H. H. Uhlig, I. I. Ivanov, D. R. Littman, K. J. Maloy, and F. Powrie. 2010. Innate lymphoid cells drive interleukin-23-dependent innate intestinal pathology. *Nature* 464: 1371–1375.
37. Izcue, A., S. Hue, S. Buonocore, C. V. Arancibia-Cárcamo, P. P. Ahern, Y. Iwakura, K. J. Maloy, and F. Powrie. 2008. Interleukin-23 restrains regulatory T cell activity to drive T cell-dependent colitis. *Immunity* 28: 559–570.
38. Fujimoto, T., K. H. Sonoda, K. Hijioka, K. Sato, A. Takeda, E. Hasegawa, Y. Oshima, and T. Ishibashi. 2010. Choroidal neovascularization enhanced by *Chlamydia pneumoniae* via Toll-like receptor 2 in the retinal pigment epithelium. *Invest. Ophthalmol. Vis. Sci.* 51: 4694–4702.
39. Yanai, H., T. Ban, Z. Wang, M. K. Choi, T. Kawamura, H. Negishi, M. Nakasato, Y. Lu, S. Hangai, R. Koshiba, et al. 2009. HMGB proteins function as universal sentinels for nucleic-acid-mediated innate immune responses. *Nature* 462: 99–103.
40. Zhang, Q., M. Raoof, Y. Chen, Y. Sumi, T. Sursal, W. Junger, K. Brohi, K. Itagaki, and C. J. Hauser. 2010. Circulating mitochondrial DAMPs cause inflammatory responses to injury. *Nature* 464: 104–107.
41. Doyle, S. L., M. Campbell, E. Ozaki, R. G. Salomon, A. Mori, P. F. Kenna, G. J. Farrar, A. S. Kiang, M. M. Humphries, E. C. Lavelle, et al. 2012. NLRP3 has a protective role in age-related macular degeneration through the induction of IL-18 by drusen components. *Nat. Med.* 18: 791–798.
42. Shichita, T., E. Hasegawa, A. Kimura, R. Morita, R. Sakaguchi, I. Takada, T. Sekiya, H. Ooboshi, T. Kitazono, T. Yanagawa, et al. 2012. Peroxiredoxin family proteins are key initiators of post-ischemic inflammation in the brain. *Nat. Med.* 18: 911–917.